Published in final edited form as:

Am J Med Genet A. 2021 July ; 185(7): 2241–2249. doi:10.1002/ajmg.a.62221.

Two novel bi-allelic *KDELR2* missense variants cause osteogenesis imperfecta with neurodevelopmental features

Stephanie Efthymiou[1], **Isabella Herman**[2,3,4], **Fatima Rahman**[5], **Najwa Anwar**[5], **Reza Maroofian**[1], **Janice Yip**[1], **Tadahiro Mitani**[3], **Daniel G. Calame**[2,3,4], **Jill V. Hunter**[6], **V. Reid Sutton**[3,4], **Elif Yilmaz Gulec**[7], **Ruizhi Duan**[3], **Jawid M. Fatih**[3], **Dana Marafi**[3,8], **Davut Pehlivan**[2,3,4], **Shalini N. Jhangiani**[3,9], **Richard A. Gibbs**[3,9], **Jennifer E. Posey**[3], **SYNAPS Study Group**[1], **Shazia Maqbool**[5], **James R. Lupski**[3,4,10,11], **Henry Houlden**[1]

[1]Department of Neuromuscular Disorders, Queen Square Institute of Neurology, University College London, London, UK

[2]Section of Pediatric Neurology and Developmental Neuroscience, Department of Pediatrics, Baylor College of Medicine, Houston, Texas

[3]Department of Molecular and Human Genetics, Baylor College of Medicine, Houston, Texas

[4]Texas Children's Hospital, Houston, Texas

[5]Development and Behavioural Pediatrics Department, Institute of Child Health and The Children Hospital, Lahore, Pakistan

[6]Division of Neuroradiology, Edward B. Singleton Department of Radiology, Texas Children's Hospital, Houston, Texas

[7]Department of Medical Genetics, Health Sciences University, Istanbul Kanuni Sultan Suleyman Research and Training Hospital, Istanbul, Turkey

[8]Department of Pediatrics, Faculty of Medicine, Kuwait University, Safat, Kuwait

[9]Human Genetics Center, University of Texas Health Science Center at Houston, Texas

[10]Human Genome Sequencing Center, Baylor College of Medicine, Houston, Texas

[11]Department of Pediatrics, Baylor College of Medicine, Houston, Texas

To the Editor:

Correspondence: Stephanie Efthymiou, Department of Neuromuscular Disorders, Queen Square Institute of Neurology, University College London, WC1N 3BG London, UK. s.efthymiou@ucl.ac.uk.
Stephanie Efthymiou and Isabella Herman contributed equally to this study.

AUTHORS' CONTRIBUTIONS

Stephanie Efthymiou and Isabella Herman performed data collection, analysis, manuscript drafting, and designed the study. Fatima Rahman, Najwa Anwar, Shazia Maqbool, Reza Maroofian, Janice Yip, Tadahiro Mitani, Daniel G. Calame, Jill V. Hunter, V. Reid Sutton, Elif Yilmaz Gulec, Ruizhi Duan, Jawid M. Fatih, Dana Marafi, Davut Pehlivan, Shalini N. Jhangiani, Richard A. Gibbs and Jennifer E. Posey organized participant recruitment and performed data collection. James R. Lupski and Henry Houlden sponsored the research, assisted in study design, and supervised the laboratory studies and clinical integration. All coauthors assisted with manuscript preparation and writing and all coauthors approved of the final manuscript.

CONFLICT OF INTEREST

The authors declare that they have no conflicts of interest.

In a recent article in the *American Journal of Human Genetics*, biallelic pathogenic *KDELR2* variants were described as a novel cause of autosomal recessive (AR) osteogenesis imperfecta (OI) (MIM: #166200) in four families with six affected individuals (van Dijk et al., 2020). The KDELR family of proteins is important in inter-organelle communication by regulating protein trafficking between the Golgi apparatus and the endoplasmic reticulum (Capitani & Sallese, 2009). *KDELR2*-related OI results from the inability of HSP47 (heat shock protein 47) to bind KDELR2, leading to failure of HSP47 to dissociate from collagen type 1. HSP47-bound extracellular collagen cannot form collagen fibers in individuals with pathogenic biallelic *KDELR2* variants (Figure 1; van Dijk et al., 2020). We read the authors' work with great enthusiasm and would like to share clinical and genetic information from two additional unrelated consanguineous families with three affected children with OI with additional phenotypic features, therefore expanding the phenotypic spectrum of *KDELR2*-related OI.

OI is a clinically and genetically heterogeneous connective tissue disorder hallmarked by increased susceptibility to bone fractures and is most commonly caused by monoallelic *de novo* pathogenic variants in *COL1A1* (MIM: 120150) or *COL1A2* (MIM: 120160). However, biallelic variants in genes involved in collagen type I biosynthesis have been frequently reported in consanguineous populations (Essawi et al., 2018; van Dijk et al., 2020; Van Dijk & Sillence, 2014). Currently, 20 different types of OI are identified in Online Mendelian Inheritance in Man (OMIM) (Amberger et al., 2015) with variable severity and phenotypic spectrum affecting primarily the skeletal system, although neurodevelopmental and other systemic complications have been observed in some autosomal recessive forms (e.g., *MESD*, MIM: 618644) (Moosa et al., 2019).

Here, we describe three affected children from two unrelated consanguineous families in order to expand the phenotype and further support the role of *KDELR2* in AR OI. Informed consent, including consent to publish photographs, was obtained from the childrens' parents and institutional review board approval was obtained. All three children were clinically diagnosed with progressively deforming OI and neurodevelopmental delay. Three children had motor delay and two of three children had speech delay. The detailed clinical features of each patient are described in Table 1. Pedigrees, radiographs, and brain magnetic resonance images (MRIs) are shown in Figure 2. Common features observed in the affected patients include musculoskeletal abnormalities, including short stature and failure to thrive, Wormian bones, bowed limbs, chest deformity, hypotonia, joint hypermobility, and dysmorphic facies (Figure 2). Family 1 consists of two affected children, a boy and a girl (P1, P2), born to consanguineous (first cousins) parents of Pakistani origin. Both patients have marked motor delay with inability to walk independently at 6 years and 2 years 8 months of age, respectively. The older child crawls as a means of ambulation and has never walked. He has had four fractures in his lifetime, the last at 4 years of age. The younger sister has not had any documented fracture to date at 2 years and 8 months of age. She is not independently ambulatory but can take few steps with great support. In addition, she has speech delay with the first word spoken recently at 2 years of age. Common dysmorphic features in both siblings include epicanthus inversus, deep, sunken eyes, short neck, and thin, sparse hair. Brain MRI obtained from P1 at 6 years of age shows brachycephaly but is otherwise unremarkable (Figure 2(e)). P3 was born to consanguineous first cousin Turkish parents

with two prior miscarriages of unknown etiology. He was prenatally suspected to have OI due to ultrasounds showing abnormal bone structure. The patient has one unaffected sibling who does not carry the variant (Figure 2). The patient's first fracture occurred at 21 days of age (Figure 2(d)). Additional features observed include dentinogenesis imperfecta, blue sclera, scoliosis, and neurodevelopmental delay involving both motor and speech. Independent ambulation and speech emerged at 2 years of age; currently at age 4 years he is comparable to his neurotypical peers. Therefore, although he may have had early childhood developmental delay with speech and motor affected, he has caught up to his peers and it is therefore difficult to dissect if the *KDELR2* variant identified contributes to the speech delay observed or if it is due to lack of exposure or other unidentified genetic etiologies. Additionally, at 4 years of age, he is currently independently ambulatory. Neurodevelopmental cognition (developmental quotient/ intelligence quotient) of all three patients is unknown nor has formal testing been performed in any of the patients.

Family-based exome sequencing (ES) with rare variant analysis was performed in both families followed by Sanger segregation for the identified variants as described before (Efthymiou et al., 2019; Manole et al., 2020). All three affected subjects were found to have homozygous variants in *KDELR2* (GenBank: NM_006854.3). P1 and P2 have a c.13C > T (p.Arg5Trp) missense variant and P3 has a c.485 A>G (p.Tyr162Cys) missense variant (Table 2). Neither variant is present in gnomAD and both variants are predicted to be pathogenic via in silico prediction analysis (CADD v1.4, MutationTaster, PolyPhen, SIFT). All current and previously reported variants affect highly conserved amino acids located in the KDELR2 transmembrane domains (Figure 1(h)).

The role of *KDELR2* in human development has not been well established until this point. However, animal studies of *KDELR2* loss of function (LoF) demonstrate an essential role in embryonic development. The characterization of *Kdelr2*-LoF mice by the International Mouse Phenotypic Consortium (IMPC)(Dickinson et al., 2016) scored several statistically significant phenotypes, including preweaning lethality, decreased animal size, bone structural abnormalities, abnormalities in head shape and size, facial dysmorphology, and abnormal body wall structure (Table 3), features which overlap with human biallelic pathogenic *KDELR2* variants.

In conclusion, the data presented here support the role of *KDELR2* in AR OI and expand the phenotypic spectrum of recessive *KDELR2*-related AR OI first described by van Dijk et al. (2020) to include neurodevelopmental disorders such as motor and speech delay, as well as blue sclerae, dentinogenesis imperfecta, and hypotonia. However, motor delay and hypotonia are common features of OI and one reason they have not previously been reported may have been due to the small sample size of patients with this newly identified genetic etiology of OI. Additionally, it is unclear if the speech delay seen in early development is related to *KDELR2*, lack of exposure, or some other unidentified etiology. Noteworthy, the phenotypic spectrum of IMPC-generated *Kdelr2*-LoF mice overlaps with human *KDELR2*-OI patients and provides a model system in which to better characterize this type of AR OI. Combined data from humans and mouse models could lead to further studies investigating the pathologic mechanism of *KDELR2*-related OI and to the development of novel disease treatments. With the current rate of novel disease gene discovery and pathogenic disease

mechanisms, it is expected that more as of yet undiscovered molecular causes of OI exist. Therefore, it becomes important to perform family-based genetic analysis in these molecular undiagnosed patients in order to work toward a diagnosis with implications for prognosis, family planning, and potential treatments to mitigate the clinical consequences of this deforming disorder.

ACKNOWLEDGMENTS

This study was supported in part by the US National Human Genome Research Institute (NHGRI) and National Heart Lung and Blood Institute (NHBLI) to the Baylor-Hopkins Center for Mendelian Genomics (BHCMG, UM1 HG006542, J.R.L); NHGRI grant to Baylor College of Medicine Human Genome Sequencing Center (U54HG003273 to R.A.G.), US National Institute of Neurological Disorders and Stroke (NINDS) (R35NS105078 to J.R.L.) and Muscular Dystrophy Association (MDA) (512848 to J.R.L.). D.M. is supported by a Medical Genetics Research Fellowship Program through the United States National Institute of Health (T32 GM007526-42). T.M. is supported by the Uehara Memorial Foundation. D.P. is supported by a Clinical Research Training Scholarship in Neuromuscular Disease partnered by the American Academy of Neurology (AAN), American Brain Foundation (ABF) and Muscle Study Group (MSG), and NIH–Brain Disorders and Development Training Grant (T32 NS043124-17). J.E.P. was supported by NHGRI K08 HG008986. Family 1 was collected as part of the SYNaPS Study Group collaboration funded by the Wellcome Trust and strategic award (Synaptopathies) funding (WT093205 MA and WT104033AIA) and research was conducted as part of the Queen Square Genomics group at University College London, supported by the National Institute for Health Research University College London Hospitals Biomedical Research Centre. HH is funded by the MRC (MR/S01165X/1, MR/S005021/1, G0601943), the National Institute for Health Research University College London Hospitals Biomedical Research Centre, Rosetree Trust, Ataxia UK, MSA Trust, Brain Research UK, Sparks GOSH Charity, Muscular Dystrophy UK (MDUK), Muscular Dystrophy Association (MDA USA).

Funding information

Medical Research Council, Grant/Award Numbers: G0601943, MR/S005021/1, MR/S01165X/1; Muscular Dystrophy Association, Grant/Award Number: 512848; National Human Genome Research Institute, Grant/Award Numbers: BHCMG, UM1 HG006542, K08 HG008986, U54HG00327; National Institute of Neurological Disorders and Stroke, Grant/Award Number: R35NS105078; NIH Clinical Center, Grant/Award Numbers: T32 GM007526-42, T32 NS043124-17; Uehara Memorial Foundation; Wellcome Trust, Grant/Award Numbers: WT093205 MA, WT104033AIA

DATA AVAILABILITY STATEMENT

The data that support the findings of this study are available from the corresponding author upon reasonable request.

REFERENCES

Amberger JS, Bocchini CA, Schiettecatte F, Scott AF, & Hamosh A (2015). OMIM.Org: Online Mendelian inheritance in man (OMIM[R]), an online catalog of human genes and genetic disorders. Nucleic Acids Research, 43, D789–D798. 10.1093/nar/gku1205 [PubMed: 25428349]

Capitani M, & Sallese M (2009). The KDEL receptor: New functions for an old protein. FEBS Letters, 583(23), 3863–3871. 10.1016/j.febslet.2009.10.053 [PubMed: 19854180]

Dickinson ME, Flenniken AM, Ji X, Teboul L, Wong MD, White JK, Meehan TF, Weninger WJ, Westerberg H, Adissu H, Baker CN, Bower L, Brown JM, Caddle LB, Chiani F, Clary D, Cleak J, Daly MJ, Denegre JM, Doe B, … Murray SA. (2016). High-throughput discovery of novel developmental phenotypes. Nature, 537(7621), 508–514. 10.1038/nature19356 [PubMed: 27626380]

Efthymiou S, Salpietro V, Malintan N, Poncelet M, Kriouile Y, Fortuna S, De Zorzi R, Payne K, Henderson LB, Cortese A, Maddirevula S, Alhashmi N, Wiethoff S, Ryten M, Botia JA, Provitera V, Schuelke M, Vandrovcova J, SYNAPS Study Group, Walsh L., … Houlden H. (2019). Biallelic mutations in neurofascin cause neurodevelopmental impairment and peripheral demyelination. Brain, 142(10), 2948–2964. 10.1093/brain/awz248 [PubMed: 31501903]

Essawi O, Symoens S, Fannana M, Darwish M, Farraj M, Willaert A, Essawi T, Callewaert B, De Paepe A, Malfait F, & Coucke PJ (2018). Genetic analysis of osteogenesis imperfecta in the Palestinian population: Molecular screening of 49 affected families. Molecular Genetics & Genomic Medicine, 6(1), 15–26. 10.1002/mgg3.331 [PubMed: 29150909]

Manole A, Efthymiou S, O'Connor E, Mendes MI, Jennings M, Maroofian R, Davagnanam I, Mankad K, Lopez MR, Salpietro V, Harripaul R, Badalato L, Walia J, Francklyn CS, Athanasiou-Fragkouli A, Sullivan R, Desai S, Baranano K, Zafar F, Rana N, … Houlden H. (2020). De novo and bi-allelic pathogenic variants in NARS1 cause neurodevelopmental delay due to toxic gain-of-function and partial loss-of-function effects. American Journal of Human Genetics, 107(2), 311–324. 10.1016/j.ajhg.2020.06.016 [PubMed: 32738225]

Moosa S, Yamamoto GL, Garbes L, Keupp K, Beleza-Meireles A, Moreno CA, Valadares ER, de Sousa SB, Maia S, Saraiva J, Honjo RS, Kim CA, Cabral de Menezes H, Lausch E, Lorini PV, Lamounier A Jr, Carniero T., Giunta C., Rohrbach M., Janner M., … Netzer C. (2019). Autosomal-recessive mutations in MESD cause osteogenesis Imperfecta. American Journal of Human Genetics, 105(4), 836–843. 10.1016/j.ajhg.2019.08.008 [PubMed: 31564437]

van Dijk FS, Semler O, Etich J, Köhler A, Jimenez-Estrada JA, Bravenboer N, Claeys L, Riesebos E, Gegic S, Piersma SR, Jimenez CR, Waisfisz Q, Flores CL, Nevado J, Harsevoort AJ, Janus G, Franken A, van der Sar AM, Meijers-Heijboer H, Heath KE, … Micha D. (2020). Interaction between KDELR2 and HSP47 as a key determinant in osteogenesis imperfecta caused by bi-allelic variants in KDELR2. American Journal of Human Genetics, 107(5), 989–999. 10.1016/j.ajhg.2020.09.009 [PubMed: 33053334]

Van Dijk FS, & Sillence DO (2014). Osteogenesis imperfecta: Clinical diagnosis, nomenclature and severity assessment. American Journal of Medical Genetics. Part A, 164A(6), 1470–1481. 10.1002/ajmg.a.36545 [PubMed: 24715559]

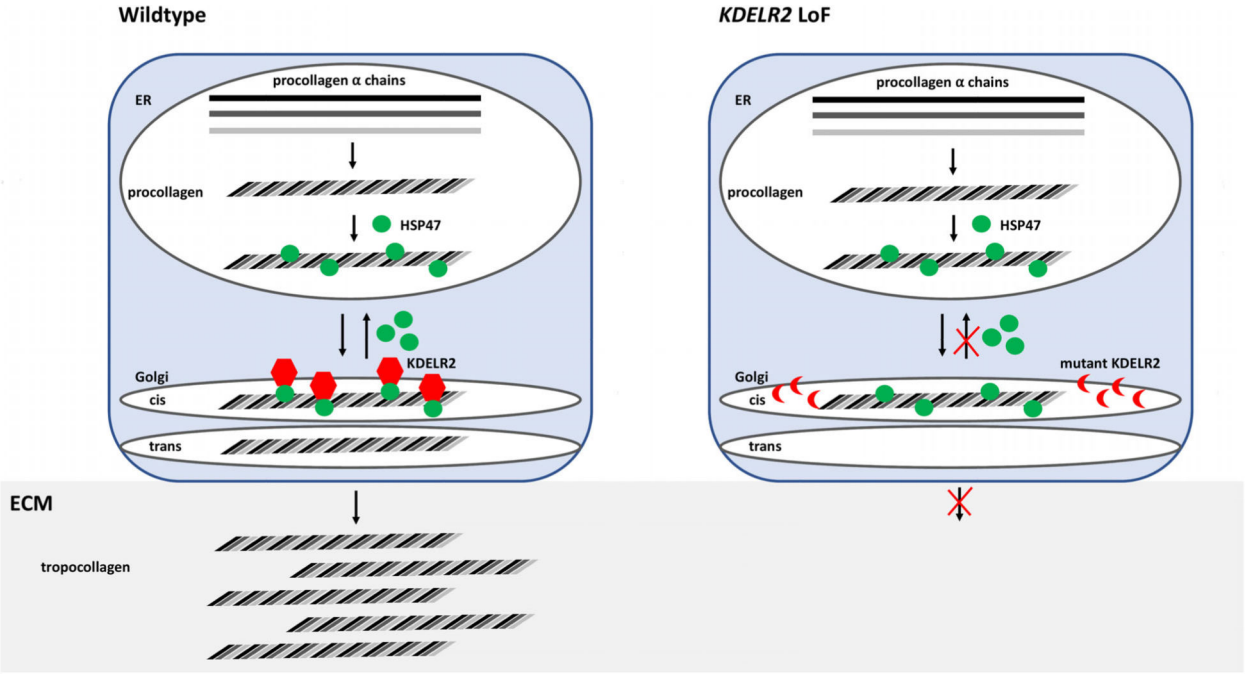

FIGURE 1.

KDELR2 loss of function (LoF) leads to inability of heat shock protein 47 (HSP47) to dissociate from procollagen. In wildtype cells, alpha collagen fibers assemble to form procollagen. Procollagen binds HSP47 and is transferred to the Golgi apparatus where KDELR2 binds HSP47 and leads to dissociation of HSP47 from procollagen. HSP47 is recycled back to the ER. Procollagen is further processed in the Golgi and secreted into the extracellular matrix (ECM) as tropocollagen. In mutant KDELR2 cells, KDELR2 is unable to bind HSP47. HSP47 cannot dissociate from procollagen and is retained in the Golgi and not secreted into the extracellular matrix

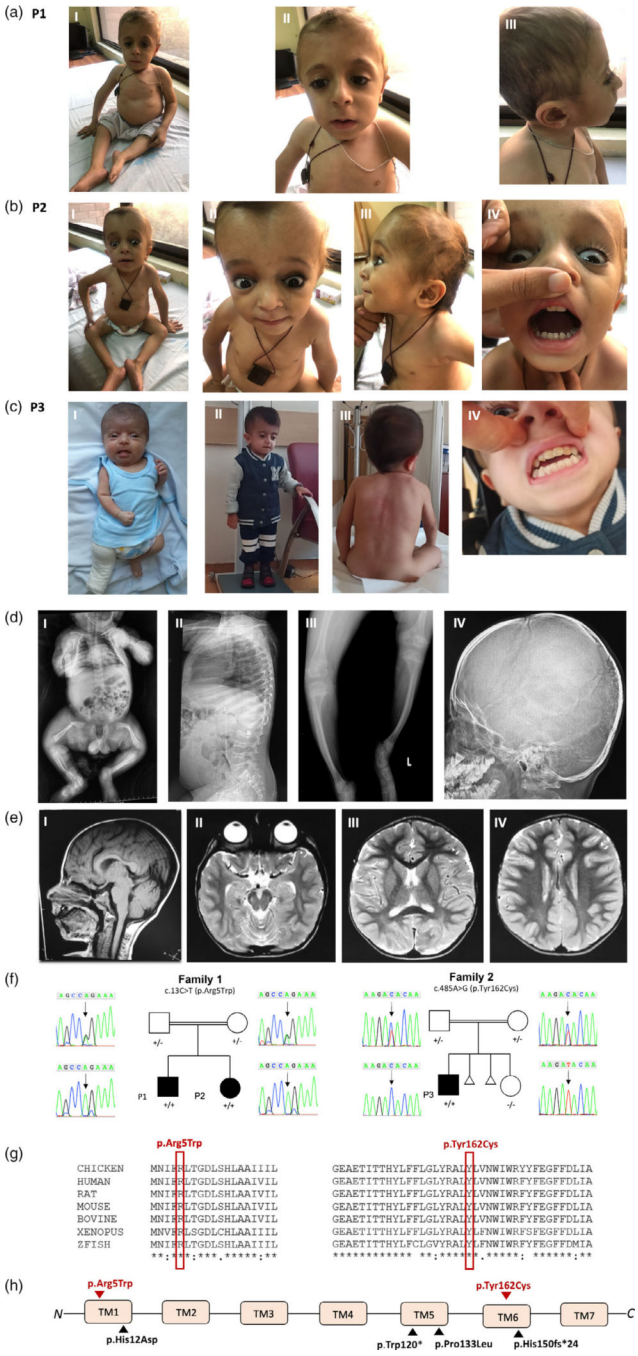

FIGURE 2.

Three affected patients with *KDELR2*-related osteogenesis imperfecta from two consanguineous families. (a) Photographs of patient P1 showing short stature, barrel shaped chest (I), sunken eyes, epicanthus inversus (II), and sparse thin hair (III). (b) Photographs of P2 showing short stature, barrel shaped chest (I), blue sclera (II), sunken eyes secondary to molding of the soft cranium (II), thin sparse hair (III), and dentinogenesis imperfecta (IV). (c) Photographs of P3 showing infantile short stature a right leg cast following a pathological femoral fracture (I), current short stature at age 4 years (II), scoliosis (III),

and dentinogenesis imperfecta (IV). (d) Radiographs of affected subjects depicting infantile femoral fracture from P3 (I), vertebral compression fractures and platyspondyly from patient P1 (II), short bowed limbs from P1 (III), and Wormian bones from P1 (IV). (e) Brain MRI sections from P1 obtained at 6 years of age. (I) Sagittal T1 showing normal brain appearance. (II) Axial T2 showing brachycephaly. (III and IV) Axial T2 images showing age-appropriate myelination. (f) Sanger segregation of *KDELR2* variants in family 1 and 2. (g) Conservation of amino acid residues across species for both variants. (h) Location of current (red) and previously reported (black) *KDELR2* pathogenic variants. All identified variants to date affect transmembrane domains (TMs) 1, 5, and 6 of the KDELR2 protein product

TABLE 1

Comparison of clinical features in patients with KDELR2-related osteogenesis imperfecta

	This study			Published in van Dijk et al., 2020					
Individual	**PI**	**P2**	**P3**	**PI**	**P2–1**	**P2–2**	**P3**	**P4–1**	**P4–2**
Ethinicity	Pakistani	Pakistani	Turkish	Pakistani	Dutch	Dutch	Spanish	Dutch	Dutch
GeneVariant (NM_006854)	C.13C > T (p.Arg5Trp) hmz	C.13C > T (p.Arg5Trp) hmz	C.485A > G (p.Tyrl62Cys) hmz	c.448dupC (p.Hisl50fs*24), hmz	c.34C > G (p.Hisl2Asp), hmz	N/A	C.398C > T (p.Prol33Leu), hmz	c.34C > G (p. Hisl2Asp), C.360G > A (p. Trpl20*)	c.34C > G (p.Hisl2Asp), C.360G > A (p.Trpl20*)
Age, first assessement	4 years 5 months	15 months	24 days	5 years	29 years	N/A	1.5 mo	24 weeks of gestation	N/A
Age, last assessment	6 years	2 years 8 months	4 years 3 months	14 years	39 years	N/A	43 years	N/A	N/A
OFC, first assessment (cm, Z-score)	47 cm (−2.5)	43 cm (−2.3)	N/A						
Height, last assessment (cm, Z-score)	77 cm (−3.1)	66.5 cm (−5.2)	83.5 cm (−3)	130 (−4.0)	121 (N/A)	115 (N/A)	138 (N/A)	N/A	N/A
Weight, last assessment (kg, Z-score)	10 kg (−3.9)	7 kg (−4.1)	10.2 kg (−3.5)	N/A	N/A	N/A	N/A	N/A	N/A
OFC, last assessment (cm, Z-score)	N/A	N/A	50.5 cm (1.1)	N/A	N/A	N/A	N/A	N/A	N/A
Prenatal fractures	U	U	+	−	−	−	−	+	+
Wormian bones	+	+	+	−	U	U	+	N/A	N/A
Age at first fracture	1 year	N/A	21 days	40	32	U	24	In utero	In utero
Estimated number of sustained fractures	4	0	>2	*N* = 12	*N* = 26	*N* = 15 aged 25 years	*N* > 30	N/A	N/A
Last sustained fracture	4 years 5 months	N/A	4 years	right femur age 10 years	right femur age 28 and right femoral neck age 29	U	right femur, age 37	N/A	N/A
Color of sclera	White	Blue	Blue	White	White	White	White	U	U
Dentinogenesis imperfecta	−	+	+	−	−	−	−	N/A	N/A
Hypermobility of joints	+	+	+	+	+	U	+	N/A	N/A

	This study			Published in van Dijk et al., 2020					
Individual	**PI**	**P2**	**P3**	**PI**	**P2–1**	**P2–2**	**P3**	**P4–1**	**P4–2**
Hearing impairment	−	−	−	−	−	−	−	N/A	N/A
Chest deformity	Barrel shaped with pectus excavatum	Bell shaped	Barrel shaped, asymmetrical mild carinatum, increased A-P diameter	Barrel shaped with pectus excavatum	Barrel shaped with pectus excavatum	+	Bell shaped	−	−
Cardiac abnormalities	−	−	mild mitral and tricuspid regurgitation	−	−	+	U	−	−
Vertebral fractures	+	−	+	+	+	U	+	N/A	N/A
Scoliosis	−	+	+	−	+	+	+	−	−
Bowing of upper extremities	+	−	−	−	+	+	+	−	−
Bowing of lower extremities	+	−	+	−	+	+	+	+	+
Shortening of upper extremities	−	−	−	−	+	+	+	+	+
Shortening of lower extremities	+	−	−	−	+	+	+	+	+
Surgical correction for bone deformation	−	−	−	+	+	+	+	N/A	N/A
Age at BP treatment (start/end)	4 years 8 months	N/A	2-month-old /still every 6 months	5/9 years	29/37 years	N/A	39/42 years	N/A	N/A
BP type and dosage	Pamidronate 0.5 mg/kg monthly for 8 months	N/A	Pamidronate 0.5 mg/kg every 6 months	Neridronate 2 mg/kg body weight, IV, every 3 months	Alendronic acid 70 mg, weekly	N/A	Zoledronate 5 mg, IV, yearly	N/A	N/A
DEXA scores before BP treatment	N/A	N/A	N/A	Z score: *L2-L4, −3.7; *TBLH, −1.9	Z score: *L2-L4, −3.09; *femoral neck (R), −2.05; *trochanter, −2.50	N/A	U: severe osteoporosis on X-rays	N/A	N/A
DEXA scores after BP treatment	N/A	N/A	N/A	Z score: *L2-L4, −2.4	Z-score: *L1-L4, −3.4	N/A	U	N/A	N/A
Calcium–level (mmol/L)	9.9	10.5	9.1	2.36	2.55	U	2.49	N/A	N/A
Individual	PI	P2	P3	PI	P2–1	P2–2	P3	P4–1	P4–2
Alkaline phosphatase at first visit (U/L)	N/A	592	261 (normal for age)	201	69	U	U	N/A	N/A

	This study			Published in van Dijk et al., 2020					
Individual	**PI**	**P2**	**P3**	**PI**	**P2–1**	**P2–2**	**P3**	**P4–1**	**P4–2**
Alkaline phosphatase at last visit (U/L)	183	368	159 (normal for age)	198	56	U	U	N/A	N/A
Vascular abnormalities	−	−	−	N/A	N/A	N/A	N/A	N/A	N/A
Skin/nail	−	−	−	N/A	N/A	N/A	N/A	N/A	N/A
MRI brain	Brachycephaly, otherwise normal	N/A	N/A, CT head was normal	N/A	N/A	N/A	N/A	N/A	N/A
Mobility	Crawls	Walks with much support	Walks independently	mobile	Wheelchair since age of 4.5 years	Wheelchair	Wheelchair since age of 18 years	N/A	N/A
Intelligence	U	U	U	Normal	Normal	Normal	Normal	N/A	N/A
Hypotonia	+	+	+	N/A	N/A	N/A	N/A	N/A	N/A
Muscle weakness	Mild	Mild	−	N/A	N/A	N/A	N/A	N/A	N/A
Speech delay	−	+	+	N/A	N/A	N/A	N/A	N/A	N/A
Motor delay	+	+	+	N/A	N/A	N/A	N/A	N/A	N/A
Family	−	−	2	N/A	N/A	N/A	N/A	N/A	N/A

Abbreviations: hmz, homozygous; U, unknown; N/A, not applicable; BP, bisphosphonate; TBLH, total body less head.

TABLE 2

Summary of pathogenic *KDELR2* variant alleles

Family	Individual	Ethnicity	Position (hgl9)	Nucleotide change	Protein dlange	Zygosity	gnomAD allele count	REVEL score	CADD score	ACMG dassification
This study										
1	Pl	Pakistani	Chr 7:6523676 G > A	c.13C > T	p.Arg5Trp	hmz	0 htz,0 hmz	0.64	35	PP1. PM2
1	P2	Pakistani	Chr 7:6523676 G > A	c.13C > T	p.Arg5Trp	hmz	0 htz,0 hmz	0.64	35	PP1. PM2
2	P3	Turkish	Chr 7:6505821 T > C	c.48SA > G	p.Tyrl62Cys	hmz	0 htz,0 hmz	0.576	32	PM2
van Dijk et al., 2020										
1	Pl	Pakistani	Chr 7:6505858 G > GG	c.448dupC	p.Hisl50fs*24	hmz	0 htz,0 hmz	–	–	PM2
2	P2-l	Dutch	Chr 7:6523655 G > C	c.34C > G	p.Hisl2Asp	hmz	0 htz,0 hmz	0.776	28	PP1, PM2
2	P2–2	Dutch	Chr 7:6523655 G > C	c.34C > G	p.Hisl2Asp	hmz	0 htz,0 hmz	0.776	28	PP1, PM2
3	P3	Spanish	Chr 7:6505908 G > A	c.398C > T	p.Pr ol33Leu	hmz	0 htz,0 hmz	0.863	30	PM2
4	P4-l	Dutch	Chr 7:6523655 G > CChr7:6505946 C > T	c.34C > G c.360G > A	p.Hisl2Asp p. Trpl20*	cmp htz	0 htz, 0 hmz 0 htz, 0 hmz	0.776; −	2841	PP1, PM2
4	P4–2	Dutch	Chr 7:6523655 G > CChr7:6505946 C > T	c.34C > G c.360G > A	p.Hisl2Asp p.Trp120*	cmp htz	0 htz, 0 hmz 0 htz,0 hmz	0.776; −	2841	PP1, PM2

Abbreviations: CADD, Combined Annotation-Dependent Depletion; cmp htz, compound heterozygous; hmz, homozygous; htz, heterozygous; REVEL, rare exome variant ensemble learner.

TABLE 3

International mouse phenotyping consortium *Kdelr2* LOF phenotypes

Phenotype	Zygosity	Life stage	*p*-value
Abnormal embryo size	htz, hmz	E9.5, E18.5	0.00
Abnormal head size	hmz	E18.5	0.00
Abnormal heart looping	htz	E.9.5	0.00
Increased exploratory behavior	htz	early adult	1.17×10^{-7}
Abnormal bone mineralization	htz	early adult	1.39×10^{-6}
Abnormal facial morphology	hmz	E18.5	0.00
Preweaning lethality, incomplete penetrance	hmz	early adult	0.00
Abnormal head shape	hmz	E18.5	0.00
Abnormal bone structure	htz	early adult	1.75×10^{-7}
Abnormal body wall morphology	hmz	E18.5	0.00

Abbreviations: hmz, homozygous; htz, heterozygous.

Am J Med Genet A. Author manuscript; available in PMC 2021 September 16.